The quadrupolar term in the equivalent crystal-field Hamiltonians for various central-ion point symmetries

2006 J. Phys. A: Math. Gen. 39 6919

(http://iopscience.iop.org/0305-4470/39/22/008)

J. Phys. A: Math. Gen. **39** (2006) 6919–6931 doi:10.1088/0305-4470/39/22/008

The quadrupolar term in the equivalent crystal-field Hamiltonians for various central-ion point symmetries

J Mulak[1] **and M Mulak**[2]

[1] W Trzebiatowski Institute of Low Temperature and Structure Research, Polish Academy of Sciences, PO Box 1410, 50-950 Wroclaw, Poland
[2] Institute of Physics, Wroclaw University of Technology, Wyb. Wyspianskiego 27, 50-370 Wroclaw, Poland

E-mail: Maciej.Mulak@pwr.wroc.pl

Received 1 January 2006
Published 16 May 2006
Online at stacks.iop.org/JPhysA/39/6919

Abstract

The method of the determination of the principal axes system (PAS) orientation with respect to the initial reference frame for any quadrupolar component of the crystal-field Hamiltonian $\mathcal{H}_{\mathrm{CF}}^{(\mathrm{II})}$ is presented. The developed method is based on the extreme points of the axial crystal-field parameter map, $B_{20}(\alpha, \beta)$, where both the partial derivatives $\partial B_{20}/\partial\alpha$ and $\partial B_{20}/\partial\beta$ simultaneously vanish, and α, β stand for the two Euler angles with respect to the initial reference frame. In general, there are three such points corresponding to a maximum, minimum and saddle point on the map. These particular points fix the orthogonal PAS in which three equivalent, two-parameter (B_{20}, B_{22}), orthorhombic-like $\mathcal{H}_{\mathrm{CF}}^{(\mathrm{II})}$ parameterizations coexist according to the three options of the z-axis. Hence, the standardization of $\mathcal{H}_{\mathrm{CF}}$ parameterizations becomes simplified and lies in the particular choice between the three forms, conventionally that with the maximal $|B_{20}|$.

PACS number: 71.70.Ch

1. Introduction

The quadrupolar term $\mathcal{H}_{\mathrm{CF}}^{(\mathrm{II})}$ is the first out of the effective components of the crystal-(ligand)-field Hamiltonians and its parameterization determines the global $\mathcal{H}_{\mathrm{CF}}$ parameterization. The complete analysis of all equivalent $\mathcal{H}_{\mathrm{CF}}^{(\mathrm{II})}$ parameterizations, i.e. those referring to various reference frames, for all point symmetries of the central ion is presented below. Throughout the paper the tensor (Wybourne [1, 2]) notation for the crystal-field Hamiltonian is consistently used. In this instance $\mathcal{H}_{\mathrm{CF}}^{(\mathrm{II})} = \sum_{q=-2}^{2} B_{2q} C_q^{(2)}$, where unprimed crystal-field parameters (CFPs) B_{2q} refer to the initial reference frame (crystallographical or nominal one [3] depending whether the initial set of CFPs is theoretical or experimentally fitted). The primed CFPs correspond to the transformed systems, and $C_q^{(2)}$ are the components of the spherical tensor operator of rank 2.

The second-order crystal-field term $\mathcal{H}_{\mathrm{CF}}^{(\mathrm{II})}$, as any second-order tensor is, in general, defined by its five components. However, according to the central-ion point symmetry reflected usually in the reference frame choice, i.e. in the so-called symmetry-adapted system, in order to parameterize the $\mathcal{H}_{\mathrm{CF}}^{(\mathrm{II})}$ one needs nominally from zero to five CFPs [4–6]. Specifically, in the case of the cubic symmetry the quadrupolar term is completely compensated and does not occur at all regardless of the choice of the reference frame. In turn, only one axial parameter, B_{20}, is needed to parameterize $\mathcal{H}_{\mathrm{CF}}^{(\mathrm{II})}$ (in its symmetry-adapted system) in the case of the axial ($C_{\infty v}$), hexagonal, tetragonal and trigonal symmetries. On the other hand, for the orthorhombic symmetry two real parameters B_{20} and B_{22} are necessary, while for the monoclinic symmetry already three: either one real B_{20} with the pair of complex-conjugate CFPs B_{22}, B_{2-2} or three real B_{20}, B_{21}, B_{22} (or one real B_{20} and two imaginary ones B_{2-1}, B_{2-2}) [7, 8]. Finally, in the case of the triclinic symmetry all five CFPs are required: one axial and two pairs of complex-conjugate $B_{2\pm1}$, $B_{2\pm2}$.

When in a given $\mathcal{H}_{\mathrm{CF}}^{(\mathrm{II})}$ parameterization a pair (or two pairs) of complex-conjugate CFPs is inherent, in our discussed case either $B_{2\pm1}$ and/or $B_{2\pm2}$, one can always reduce the number of the CFPs by one appropriately rotating the initial reference frame about its z-axis [9, 10]. In this way, any monoclinic $\mathcal{H}_{\mathrm{CF}}^{(\mathrm{II})}$ can always be reduced to the form characteristic for the orthorhombic $\mathcal{H}_{\mathrm{CF}}^{(\mathrm{II})}$. But, interestingly, this is only a prelude to the main property of the quadrupolar term—the general possibility of the so-called diagonalization of $\mathcal{H}_{\mathrm{CF}}^{(\mathrm{II})}$ [3, 11, 12].

However, having just a formal regard for the crystallographical point symmetry of the central ion does not confine further possible reduction in the number of the CFPs needed for the quadrupolar potential parameterization. An infinite number of arbitrary rotations of the reference frame, naturally followed by the loss of potential advantages of the symmetry-adapted system, lead to an infinite number of equivalent $\mathcal{H}_{\mathrm{CF}}^{(\mathrm{II})}$ parameterizations. Nevertheless, there exists among them a certain particular form. The quadrupolar term $\mathcal{H}_{\mathrm{CF}}^{(\mathrm{II})}$ for mono- or triclinic central-ion point symmetry can always be reduced to the form in which at most two real CFPs, B'_{20} and B'_{22}, are essential. It may be achieved by way of the diagonalization of $\mathcal{H}_{\mathrm{CF}}^{(\mathrm{II})}$ [3, 11, 12], i.e. rotating the initial reference system to the principal axes system (PAS) by a unique set of Euler angles (α, β, γ) [13–15]. And so, the first angle α refers to the rotation about the original z-axis, the second β about the new (transformed) y-axis and the third γ, in the case of need, about the final direction of the z-axis.

This paper presents a direct calculational method of finding the PAS with respect to the initial reference frame for any original low-symmetry $\mathcal{H}_{\mathrm{CF}}^{(\mathrm{II})}$ parameterization being characterized by $x_1 = \frac{|B_{21}|}{B_{20}}$, $x_2 = \frac{|B_{22}|}{B_{20}}$ and the phases φ_1 and φ_2 of its complex-conjugate CFPs, respectively. The three axes of the PAS correspond to such three directions of the z-axis of the system obtained through rotation of the initial system by $(\alpha, \beta, 0)$ Euler angles, for which both $\partial B'_{20}/\partial\alpha$ and $\partial B'_{20}/\partial\beta$ simultaneously become zero, i.e. to a maximum, minimum and saddle point on the $B'_{20}(\alpha, \beta)$ map [14, 15]. The exact calculational method how to get the direction cosines of the principal axes is developed in section 2. Further, some chosen instructive limiting cases (x_1 and/or x_2 equal to zero), which require separate investigations due to their indeterminacy, are discussed in subsection 2.1. The introduced formalism is illustrated by an example of the $\mathcal{H}_{\mathrm{CF}}^{(\mathrm{II})}$ term for the U^{4+} ion of the C_1 point symmetry in UF_4 [15, 16]. Section 3, in turn, covers the relationships between the three distinguished pairs of the CFPs $B_{20}^{(i)}$, $B_{22}^{(i)}$, $i = 1, 2, 3$, corresponding to the three choices of the z-axis within the PAS, as well as the connections between the $x_2^{(i)}$ ratios within their triads. It should be emphasized that the method presented in this paper is innately related to the method of standardization of the equivalent $\mathcal{H}_{\mathrm{CF}}$ parameterizations which is based on the transformation of their quadrupolar component and has been introduced by Rudowicz 20 years ago [3, 7, 8]. In order to clearly approach the concept of the PAS and to throw a new light on the standardization idea of $\mathcal{H}_{\mathrm{CF}}$ parameterizations some model orthorhombic coordinations generating quadrupolar $\mathcal{H}_{\mathrm{CF}}^{(\mathrm{II})}$ terms of various x_2 ratios are considered in section 4. The conclusions comprised in section 5 are completed with the open but inevitable question: is there any correlation between the local coordination geometry of the central ion and the relevant PAS?

2. Transformation of the initial reference frame of $\mathcal{H}_{\mathrm{CF}}^{(\mathrm{II})}$ into its principal axes system

Under the notion of the initial reference frame we understand either a crystallographical or nominal [3] reference system, depending whether we deal with any theoretical or fitted initial set of CFPs to be transformed. Let us consider a general case of $\mathcal{H}_{\mathrm{CF}}^{(\mathrm{II})}$ parameterization expressed by a set of five CFPs $B_{kq}(k = 2, q = 0, \pm 1, \pm 2)$, typical for the complete parameterization (C-approach [7]) of the triclinic $\mathcal{H}_{\mathrm{CF}}^{(\mathrm{II})}$. The higher symmetry $\mathcal{H}_{\mathrm{CF}}^{(\mathrm{II})}$ parameterizations become particular cases of this general one. Then,

$$\mathcal{H}_{\mathrm{CF}}^{(\mathrm{II})} = B_{20}C_0^{(2)} + B_{21}C_1^{(2)} + B_{2-1}C_{-1}^{(2)} + B_{22}C_2^{(2)} + B_{2-2}C_{-2}^{(2)},$$

where $C_q^{(2)} \equiv \sum_i C_q^{(2)}(\theta_i, \phi_i)$, and θ_i, ϕ_i stand for the polar angular coordinates of the open-shell electrons (i).

Due to the rotation of the initial reference frame by two Euler angles $(\alpha, \beta, 0)$, the axial CFP B_{20} takes the following form [13, 15, 17]:

$$\begin{aligned} B'_{20} &= C_0^{(2)}(\alpha,\beta)B_{20} + C_1^{(2)}(\alpha,\beta)B_{21} + C_{-1}^{(2)}(\alpha,\beta)B_{2-1} + C_2^{(2)}(\alpha,\beta)B_{22} + C_{-2}^{(2)}(\alpha,\beta)B_{2-2} \\ &= C_0^{(2)}(\beta)B_{20} + 2C_1^{(2)}(\beta)|B_{21}|\cos(\alpha+\varphi_1) + 2C_2^{(2)}(\beta)|B_{22}|\cos 2(\alpha+\varphi_2), \end{aligned}$$

where $B_{21} = |B_{21}|\,\mathrm{e}^{\mathrm{i}\varphi_1}$, $B_{2-1} = -|B_{21}|\,\mathrm{e}^{-\mathrm{i}\varphi_1}$, $B_{22} = |B_{22}|\,\mathrm{e}^{2\mathrm{i}\varphi_2}$, $B_{2-2} = |B_{22}|\,\mathrm{e}^{-2\mathrm{i}\varphi_2}$ are the initial CFPs, whereas $C_0^{(2)}(\beta) = \frac{1}{2}(3\cos^2\beta - 1)$, $C_1^{(2)}(\beta) = \frac{\sqrt{6}}{2}\sin\beta\cos\beta$, $C_2^{(2)}(\beta) = \frac{\sqrt{6}}{4}\sin^2\beta$ [13, 17]. Thus,

$$B'_{20} = \left[\tfrac{1}{2}(3\cos^2\beta - 1) + \sqrt{6}x_1\sin\beta\cos\beta\cos(\alpha+\varphi_1) + \tfrac{\sqrt{6}}{2}x_2\sin^2\beta\cos 2(\alpha+\varphi_2)\right]B_{20}, \tag{1}$$

where $x_1 = \frac{|B_{21}|}{B_{20}}$ and $x_2 = \frac{|B_{22}|}{B_{20}}$. Similarly, using the remaining rows of the $\mathcal{D}^{(2)}$ matrix [13, 17] one gets

$$\begin{aligned} B'_{21} = \Big\{&(-\sqrt{6}/4)\sin 2\beta + x_1\cos 2\beta\cos(\alpha+\varphi_1) + \tfrac{1}{2}x_2\sin 2\beta\cos 2(\alpha+\varphi_2) \\ &+ \mathrm{i}[x_1\cos\beta\sin(\alpha+\varphi_1) + x_2\sin\beta\sin 2(\alpha+\varphi_2)]\Big\}B_{20} \end{aligned} \tag{2}$$

and

$$\begin{aligned} B'_{22} = \Big\{&(\sqrt{6}/4)\sin^2\beta - \tfrac{1}{2}x_1\sin 2\beta\cos(\alpha+\varphi_1) + x_2\left(1 - \tfrac{1}{2}\sin^2\beta\right)\cos 2(\alpha+\varphi_2) \\ &+ \mathrm{i}[-x_1\sin\beta\sin(\alpha+\varphi_1) + x_2\cos\beta\sin 2(\alpha+\varphi_2)]\Big\}B_{20}. \end{aligned} \tag{3}$$

Naturally, the modulus $M_2 = \left[\sum_q |B'_{2q}|^2\right]^{1/2}$ is invariant under arbitrary rotation of the reference frame.

The distinguished points on the $B'_{20}(\alpha, \beta)$ map are those for which both the first partial derivatives simultaneously vanish

$$\frac{\partial B'_{20}}{\partial \alpha} = -\sqrt{6}\sin\beta[x_1\cos\beta\sin(\alpha+\varphi_1) + x_2\sin\beta\sin 2(\alpha+\varphi_2)]B_{20} \tag{4}$$

and

$$\frac{\partial B'_{20}}{\partial \beta} = \sqrt{6}\left[-\frac{\sqrt{6}}{4}\sin 2\beta + x_1\cos 2\beta\cos(\alpha+\varphi_1) + \frac{1}{2}x_2\sin 2\beta\cos 2(\alpha+\varphi_2)\right]B_{20}. \tag{5}$$

According to the report by Burdick and Reid in [14], which is valid not only for $k = 2$, the vanishing of the derivatives (equations (4) and (5)) leads to the disappearance of the $B_{2\pm1}$ CFPs (equation (2)), however with one reservation. Substituting equations (4) and (5) into equation (2), we have

$$B'_{21} = \frac{1}{\sqrt{6}}\frac{\partial B'_{20}}{\partial \beta} - \frac{\mathrm{i}}{\sqrt{6}\sin\beta}\frac{\partial B'_{20}}{\partial \alpha}. \tag{6}$$

Consequently, when $\beta = 0$ or π, i.e. when the initial z-axis direction is conserved, the second term in equation (6) becomes indeterminate of the $0/0$ type. But then, as results from equation (4), $\frac{\partial B'_{20}}{\partial \alpha} \equiv 0$, while $\frac{\partial B'_{20}}{\partial \beta} = 0$ if $\cos(\alpha+\varphi_1) = 0$, regardless of the x_1 value ($x_1 \neq 0$) (equation (5)). And so we have on the $B'_{20}(\alpha, \beta)$ map a distinguished saddle point $\left(\alpha = \frac{\pi}{2} - \varphi_1, \beta = 0\right)$ which corresponds to the initial z-axis direction established by the choice of the initial reference frame. Generally, this specific point does not enter the triad of the true distinguished points fixing the PAS (see section 3). The $B'_{2\pm1}$ CFPs do not vanish at this apparent saddle point, but according to the rotation by α angle (equation (2)) one has $B'_{2\pm1} = \pm\mathrm{i}|B_{21}|$. In the case of a real B_{21} CFP ($\varphi_1 = 0$), this apparent distinguished point always has the coordinates $\left(\frac{\pi}{2}, 0\right)$. If $x_1 = 0$ then the point $(0, 0)$, representing all the α-axis points, plays a role of the true distinguished point—the z-axis is now one out of the three principal axes.

Let us consider the true distinguished points in the general case, i.e. for $\beta \neq 0$. Then,

$$-\sqrt{6}\sin\beta[x_1\cos\beta\sin(\alpha+\varphi_1) + x_2\sin\beta\sin 2(\alpha+\varphi_2)] = 0 \tag{7}$$

$$-3\sin\beta\cos\beta + \sqrt{6}x_1(\cos^2\beta - \sin^2\beta)\cos(\alpha+\varphi_1) + \sqrt{6}x_2\sin\beta\cos\beta\cos 2(\alpha+\varphi_2) = 0. \tag{8}$$

From equation (7) results

$$\tan\beta = -\frac{x_1\sin(\alpha+\varphi_1)}{x_2\sin 2(\alpha+\varphi_2)},$$

and hence

$$\beta = \arctan\left[-\frac{x_1\sin(\alpha+\varphi_1)}{x_2\sin 2(\alpha+\varphi_2)}\right] \pm \pi. \tag{9}$$

In turn, from equation (8) one gets

$$\tan 2\beta = -\frac{-2x_1\cos(\alpha+\varphi_1)}{x_2\cos 2(\alpha+\varphi_2) - \frac{\sqrt{6}}{2}},$$

and hence

$$\beta = \frac{1}{2}\arctan\left[\frac{-2x_1\cos(\alpha+\varphi_1)}{x_2\cos 2(\alpha+\varphi_2) - \frac{\sqrt{6}}{2}}\right] \pm \frac{\pi}{2}. \tag{10}$$

For the specified initial parameters, $x_1, x_2, \varphi_1, \varphi_2$, the true distinguished points on the $B'_{20}(\alpha, \beta)$ map corresponding to its maximum, minimum and saddle point are the intersection points of both the $\beta(\alpha)$ functions (equations (9) and (10)). These points fix the directions of the three axes of certain particular reference system called the principal axes system (PAS) [3, 11, 12]. There are always three such solutions which refer to the three axes of the PAS except for the purely axial $\mathcal{H}_{\mathrm{CF}}^{(\mathrm{II})}$, $x_1 = 0$ and $x_2 = 0$, for which an infinite number of such solutions exist instead of two distinguished ones (there is a line of such distinguished points), but no saddle point occurs (subsection 2.1).

The orthogonality of the axes found in the above way can be confirmed directly using the expression for the angle between the vectors and knowing their angles $\alpha^{(i)}, \beta^{(i)}$ for $i = 1, 2, 3$ [15]. This orthogonality can also be proved generally. Let us choose one out of the distinguished directions, e.g. that with $i = 1$ as a starting point. The relevant x- and y-axes orientation can be taken so as to make the $B_{22}^{(1)}$ CFP real, i.e. to put $\varphi_2 = 0$ without any loss of generality. So, the pair of real CFPs $B_{20}^{(1)}$ and $B_{22}^{(1)}$ are given as the input data. Let us now define the rotational transformations leading to some other reference systems in which the $B'_{2\pm1}$ CFPs vanish as well. From equation (2) results that the real part of these CFPs disappears for $\sin 2\beta = 0$ ($x_1 = 0$ is assumed) and their imaginary part for $\sin 2\beta = 0$ or $\sin 2\alpha = 0$, respectively. Consequently, these are the reference systems after the following rotations of the initial system:

$$\begin{aligned}
&(1)\quad \alpha = 0 \text{ (as an arbitrary choice)}, \qquad \beta = 0\text{— for the chosen direction } (i = 1),\\
&(2)\quad \alpha = 0, \qquad \beta = \frac{\pi}{2}\text{— for the second distinguished direction } (i = 2),\\
&(3)\quad \alpha = \frac{\pi}{2}, \qquad \beta = \frac{\pi}{2}\text{— for the third distinguished direction } (i = 3).
\end{aligned} \tag{11}$$

In fact, as implies from equations (4) and (5) both the derivatives $\partial B'_{20}/\partial\alpha$ and $\partial B'_{20}/\partial\beta$ are equal to zero after the above three rotations, and thus the specified directions are orthogonal (expressions (11)). Moreover, the $B_{22}^{(2)}$ and $B_{22}^{(3)}$ CFPs remain real (equation (3)). These directions are the principal axes.

As an example, the second-order $\mathcal{H}_{\mathrm{CF}}^{(\mathrm{II})}$ term for U^{4+} ion of the C_1 site symmetry in UF_4 [15, 16] is considered below in details. The complete set of the five theoretical second-order CFPs (given in the last column of table IV in [16]) was estimated as (in cm^{-1}): $B_{20} = 526$, $|B_{21}| = 298$, $\varphi_1 = -32.5°$, $|B_{22}| = 948$, $\varphi_2 = -69.0°$. So, $x_1 = 0.567$, $x_2 = 1.802$ and $M_2 = 1501$. Employing equations (9) and (10) the corresponding diagram can be plotted (figure 1). The triad of points 1, 2, 3 refers to the PAS for the considered $\mathcal{H}_{\mathrm{CF}}^{(\mathrm{II})}$. Due to the independence of the axial B_{20} CFP on the z-axis sense, the (α, β) points are duplicated as $(\alpha + \pi, \pi - \beta)$ points seen as $1', 2', 3'$ triad in figure 1.

2.1. *The particular limiting cases of $\mathcal{H}_{\mathrm{CF}}^{(\mathrm{II})}$ parameterizations*

For certain values of the parameters x_1, x_2, φ_1 and φ_2, the right-hand sides of equations (9) and (10) can take the indeterminate forms which need an individual examination. It is instructive to focus on the following particular cases:

$$(1)\ x_1 = \frac{|B_{21}|}{B_{20}} = 0, \qquad (2)\ x_2 = \frac{|B_{22}|}{B_{20}} = 0, \qquad (3)\ x_1 = x_2 = 0.$$

In the first case,

$$\frac{\partial B'_{20}}{\partial\alpha} = -\sqrt{6}x_2 \sin^2\beta \sin 2(\alpha + \varphi_2) B_{20}$$

$$\frac{\partial B'_{20}}{\partial\beta} = \sin\beta\cos\beta[-3 + \sqrt{6}x_2 \cos 2(\alpha + \varphi_2)] B_{20}.$$

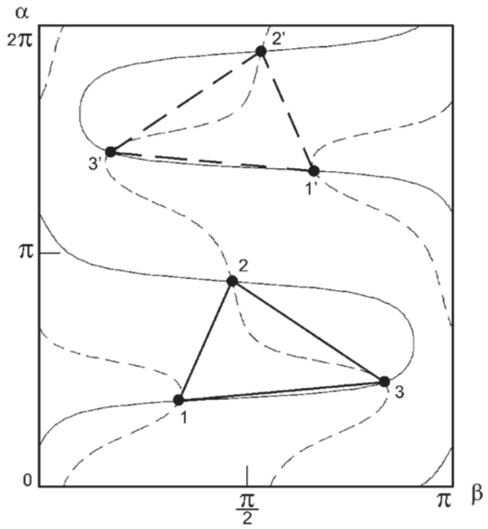

Figure 1. The diagram of the distinguished points (directions) on the $B'_{20}(\alpha, \beta)$ map of $\mathcal{H}_{\rm CF}^{\rm (II)}$ for U^{4+} ion of the C_1 point symmetry in UF_4 [15, 16]. The points of the solid lines satisfy equation (9) and those of the dashed lines equation (10). The intersection points correspond to the distinguished directions: (1) maximum (1064 cm^{-1}) ($\alpha = 66.2°$, $\beta = 60.6°$); (2) minimum (-1448 cm^{-1}) ($\alpha = 159.8°$, $\beta = 83.6°$); (3) saddle point (384 cm^{-1}) ($\alpha = 80.8°$, $\beta = 149.7°$).

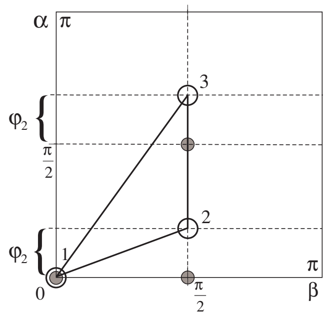

Figure 2. The position of the three principal axes 1, 2, 3 on the $B'_{20}(\alpha, \beta)$ map of $\mathcal{H}_{\rm CF}^{\rm (II)}$ with $x_1 = 0$ ($\varphi_2 < 0$ option) with respect to the initial reference frame. This triad is marked by the triangle of circles. The solid points denote the standard axes positions, i.e. when $\varphi_2 = 0$ in the initial reference frame.

The initial parameterization form proves that its reference system z-axis belongs to the principal axes. The distinguished points on the $B'_{20}(\alpha, \beta)$ map within the ranges $0 \leqslant \alpha < \pi$ and $0 \leqslant \beta < \pi$ now have the coordinates (figure 2) (1) $\alpha = 0$ (as an arbitrary choice), $\beta = 0$; (2) $\alpha = -\varphi_2, \beta = \frac{\pi}{2}$; (3) $\alpha = \frac{\pi}{2} - \varphi_2, \beta = \frac{\pi}{2}$. Rotating the initial frame about its z-axis by φ_2 angle, which corresponds to the transformation of the $B_{2\pm2}$ CFPs to their real form, yields the standard PAS arrangement on the map. Such an arrangement forming a right-angled isosceles triangle is independent of the x_2 ratio and, in consequence, is common for all $\mathcal{H}_{\rm CF}^{\rm (II)}$ parameterizations (expressed in their symmetry-adapted system) of orthorhombic and monoclinic (after the rotation by φ_2) symmetries.

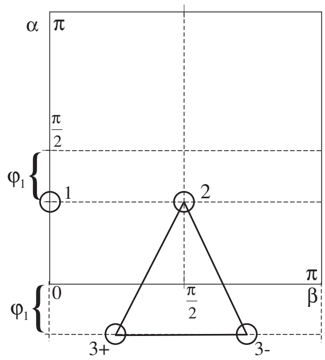

Figure 3. The position of the three principal axes 2, 3+, 3− on the $B'_{20}(\alpha, \beta)$ map of $\mathcal{H}_{\mathrm{CF}}^{(\mathrm{II})}$ with $x_2 = 0$ ($\varphi_1 > 0$ option) with respect to the initial reference frame. The additional apparent distinguished point 1 corresponds to the initial z-axis direction.

In the second case, we get

$$\frac{\partial B'_{20}}{\partial \alpha} = -\sqrt{6}x_1 \sin\beta \cos\beta \sin(\alpha + \varphi_1) B_{20}$$

$$\frac{\partial B'_{20}}{\partial \beta} = [-3\sin\beta\cos\beta + \sqrt{6}x_1(\cos^2\beta - \sin^2\beta)\cos(\alpha + \varphi_1)]B_{20},$$

and the distinguished points (within the ranges $0 \leqslant \alpha < \pi$ and $0 \leqslant \beta < \pi$) are displayed in figure 3:

$$(1) \quad \alpha = \frac{\pi}{2} - \varphi_1, \quad \beta = 0;$$

$$(2) \quad \alpha = \frac{\pi}{2} - \varphi_1, \quad \beta = \frac{\pi}{2};$$

$$(3) \quad \alpha = -\varphi_1, \quad \beta = \pm\frac{1}{2}\arctan\frac{2\sqrt{6}}{3}x_1.$$

Here, in figure 3, the characteristic feature of the PAS is the horizontal (3+, 3−) base orientation of the isosceles triangle 2, 3+, 3−, which is symmetrical itself respective to the $\beta = \frac{\pi}{2}$ line.

Finally, in the third case for $B'_{20} = \frac{1}{2}(3\cos^2\beta - 1)B_{20}$ the derivatives simplify considerably:

$$\frac{\partial B'_{20}}{\partial \alpha} \equiv 0, \qquad \frac{\partial B'_{20}}{\partial \beta} = -\frac{3}{2}\sin 2\beta B_{20},$$

and now the distinguished points form in figure 4 the straight lines with either $\beta = 0$ (maximum for $B_{20} > 0$) or $\beta = \frac{\pi}{2}$ (minimum). Due to the $\mathcal{H}_{\mathrm{CF}}^{(\mathrm{II})}$ axial symmetry ($C_{\infty,v}$) respective to the initial z-axis, the perpendicular distinguished directions do not depend on α angle. The saddle point cannot occur since for $\beta = 0$ and $\beta = \frac{\pi}{2}$ we have $B'_{20} = B_{20}$ and $B'_{20} = -\frac{1}{2}B_{20}$, respectively. The direct transformational relationship between the considered parameterization and those with $x_2 = \pm\frac{\sqrt{6}}{2}, x_1 = 0$ can be revealed since these three parameterizations correspond to the various axes of the particular PAS (figure 4).

For $x_2 = \frac{\sqrt{6}}{2}$,

$$\frac{\partial B'_{20}}{\partial \alpha} = -6\sin^2\beta \sin(\alpha + \varphi_2)\cos(\alpha + \varphi_2) B_{20}$$

$$\frac{\partial B'_{20}}{\partial \beta} = -6\sin\beta\cos\beta\sin^2(\alpha + \varphi_2) B_{20},$$

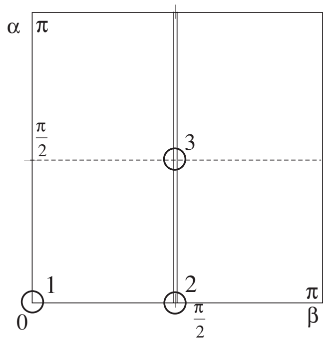

Figure 4. The distinguished points forming the lines $\beta = 0$ and $\beta = \frac{\pi}{2}$ on the map $B'_{20}(\alpha, \beta) = \frac{1}{2}(3\cos^2\beta - 1)B_{20}$. All the directions perpendicular to the initial z-axis are distinguished but equivalent, so no saddle point occurs. The triad 1, 2, 3 determines the representative PAS.

and, in consequence, the distinguished points are (any α, $\beta = 0$) and $\underline{(\alpha = -\varphi_2, \text{any } \beta)}$.

For $x_2 = -\frac{\sqrt{6}}{2}$,

$$\frac{\partial B'_{20}}{\partial \alpha} = 6\sin^2\beta \sin(\alpha + \varphi_2)\cos(\alpha + \varphi_2)B_{20}$$

$$\frac{\partial B'_{20}}{\partial \beta} = -6\sin\beta\cos\beta\cos^2(\alpha + \varphi_2)B_{20},$$

with the distinguished points given by (any α, $\beta = 0$) and $\underline{(\alpha = \frac{\pi}{2} - \varphi_2, \text{any}\beta)}$. The underlined second solutions show their independence on the β angle due to the $(C_{\infty,v})$ symmetry of the $\mathcal{H}_{\mathrm{CF}}^{(\mathrm{II})}$ in relation to the x- and y-axes, respectively.

3. Relationships between the CFPs and their ratios for three possible choices of the z-axis in the PAS

A chosen distinguished direction (one out of the three principal axes), e.g. for $i = 1$, determines the definite angles $\alpha^{(1)}$, $\beta^{(1)}$ of the rotation with respect to the initial reference frame. Hence,

$$B_{20}^{(1)} = \left[\frac{1}{2}(3\cos^2\beta^{(1)} - 1) + \sqrt{6}x_1 \sin\beta^{(1)}\cos\beta^{(1)}\cos(\alpha^{(1)} + \varphi_1) \right.$$
$$\left. + \frac{\sqrt{6}}{2}x_2\sin^2\beta^{(1)}\cos 2(\alpha^{(1)} + \varphi_2)\right]B_{20},$$

and

$$B_{22}^{(1)} = \pm\left\{\frac{1}{2}\left[M_2^2 - \left(B_{20}^{(1)}\right)^2\right]\right\}^{1/2},$$

where the signs $\pm$ refer either to the first or second kind of orthorhombic symmetry [18]. The $B_{22}^{(1)}$ CFP can also be calculated immediately based on equation (3) for the applied angles of rotation $\alpha^{(1)}$, $\beta^{(1)}$. Then, its real value amounts to

$$B_{22}^{(1)} = \pm\Big\{\Big[(\sqrt{6}/4)\sin^2\beta^{(1)} - \tfrac{1}{2}x_1\sin 2\beta^{(1)}\cos(\alpha^{(1)}+\varphi_1) + x_2\left(1-\tfrac{1}{2}\sin^2\beta^{(1)}\right)\cos 2(\alpha^{(1)}+\varphi_2)\Big]^2 + [-x_1\sin\beta^{(1)}\sin(\alpha^{(1)}+\varphi_1) + x_2\cos\beta^{(1)}\sin 2(\alpha^{(1)}+\varphi_2)]^2\Big\}^{1/2} B_{20}.$$

Substituting the rotation angles (expressions (11)) into equations (1) and (3), the following relationships hold for the remaining two distinguished directions ($i = 2, 3$):

$$B_{20}^{(2)} = -\tfrac{1}{2}B_{20}^{(1)} + \tfrac{\sqrt{6}}{2}B_{22}^{(1)}, \qquad B_{22}^{(2)} = \pm\left(\tfrac{\sqrt{6}}{4}B_{20}^{(1)} + \tfrac{1}{2}B_{22}^{(1)}\right)$$

and

$$B_{20}^{(3)} = -\tfrac{1}{2}B_{20}^{(1)} - \tfrac{\sqrt{6}}{2}B_{22}^{(1)}, \qquad B_{22}^{(3)} = \pm\left(\tfrac{\sqrt{6}}{4}B_{20}^{(1)} - \tfrac{1}{2}B_{22}^{(1)}\right). \tag{12}$$

Between the CFPs $B_{20}^{(i)}$ and $B_{22}^{(i)}$, $i = 1, 2, 3$, apart from the obvious relations $\left(B_{20}^{(i)}\right)^2 + 2\left(B_{22}^{(i)}\right)^2 = M_2^2$, other connections are fulfilled as well:

$$\sum_{i=1}^{3} B_{20}^{(i)} = 0, \qquad \sum_{i=1}^{3}\left[B_{20}^{(i)}\right]^2 = \sum_{i=1}^{3}\left[B_{22}^{(i)}\right]^2 = \frac{3}{2}M_2^2.$$

In consequence, the sum of two smaller absolute values among the three $\left|B_{22}^{(i)}\right|$ is equal to the third largest modulus. The saddle point is characterized by the largest $\left|B_{22}^{(i)}\right|$ value. In the example discussed above (U^{4+} ion of the C_1 point symmetry in UF_4), the CFPs values $B_{22}^{(1)} = 748$, $B_{22}^{(2)} = 279$ and $B_{22}^{(3)} = 1026$ in cm^{-1} confirm the previous relationships. They are also fulfilled by the results of Burdick and Reid [14].

Let us now analyse the relationships between the ratios $x_2^{(i)} = B_{22}^{(i)}/B_{20}^{(i)}$. According to equation (12)

$$x_2^{(2)} = \pm\frac{1}{\sqrt{6}}\left(1 - \frac{4}{1-\sqrt{6}x_2^{(1)}}\right)$$
$$x_2^{(3)} = \pm\frac{1}{\sqrt{6}}\left(1 - \frac{4}{1+\sqrt{6}x_2^{(1)}}\right). \tag{13}$$

The values $\left|B_{20}^{(i)}\right|/M_2$ that correspond to any triad $x_2^{(1)}, x_2^{(2)}, x_2^{(3)}$ can be found from the plots 1, 2, 3 in figure 5, where the values for an optional triad (2.000, 0.827, 0.131) are marked. The three $\left|B_{20}^{(i)}\right|/M_2$ values for all the three $x_2^{(i)}$ from a triad are equal but they belong to different plots (figure 5). For a chosen triad (2.000, 0.827, 0.131), the maximum corresponds to the plots 3, 3, 1, respectively. Similarly, the minimum to the plots 2, 1, 3 and the saddle point to the plots 1, 2, 2.

As seen from the diagram in figure 5, the maximal value of $\left|B_{20}^{(i)}\right|/M_2$, i.e. the largest one within the PAS, $\max\left|B_{20}^{(i)}\right|/M_2$, $i = 1, 2, 3$, cannot be less than 0.8660. Within the range $|x_2| \leqslant 2$ its average magnitude amounts to 0.974. This evident proximity of $\max\left|B_{20}^{(i)}\right|/M_2$ value to 1 suggests the possibility of a rough approximation, i.e. taking in a preliminary fitting procedure only the purely axial $\mathcal{H}_{CF}^{(II)}$ with all the consequences of that.

There are two particular triads $\left(0, \pm\frac{\sqrt{6}}{2}, \pm\frac{\sqrt{6}}{2}\right)$ and $\left(\infty, \pm\frac{1}{\sqrt{6}}, \pm\frac{1}{\sqrt{6}}\right)$ which have either characteristic intersection points of the plots or display asymptotic convergence to each other for $x_2 \to \infty$ (figure 5). The first triad refers to the purely axial $(C_{\infty,v})\mathcal{H}_{CF}^{(II)}$ (or an axial one if the axial multiplicity exceeds 2), when for the three ratios of the triad $\max\left|B_{20}^{(i)}\right|/M_2 = 1$, and the distinguished directions are successively the z-, x- and y-axes with

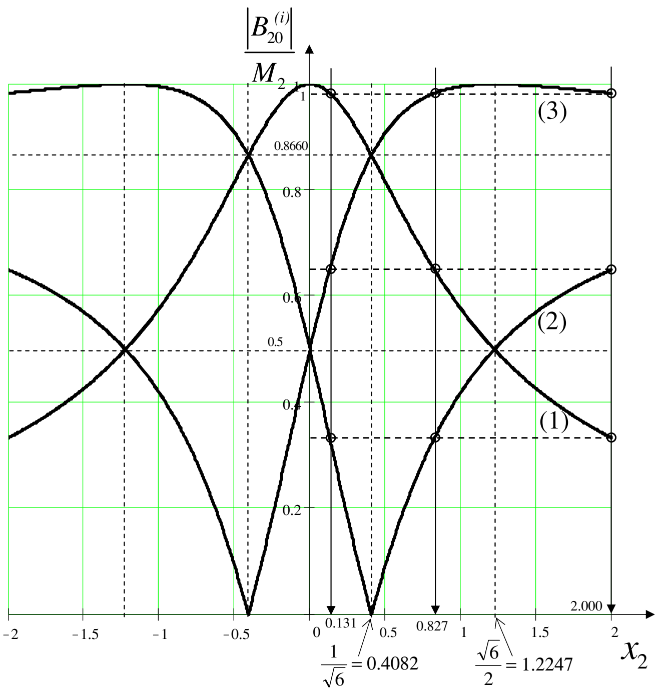

Figure 5. The $\frac{|B_{20}^{(i)}|}{M_2}$ versus x_2 plots, where $i = 1, 2, 3$ runs over the three principal axes. An optional x_2 triad (2.000, 0.827, 0.131) is shown.

all the directions perpendicular to them, respectively (see subsection 2.1). In turn, the second triad can be, e.g., associated with the $\mathcal{H}_{\mathrm{CF}}^{(\mathrm{II})}$ of the rectangle of ligands with the coordinates $\theta = \pm \arccos \frac{1}{\sqrt{3}}$, $\phi = 0$ (see section 4).

The possibility of grouping of all x_2 ratios into their separate triads (equation 13) is the key feature of the second-order tensors conditioning the PAS and enabling their diagonalization. In general, the higher order multipoles do not possess this property.

4. Some model orthorhombic coordinations yielding quadrupolar terms $\mathcal{H}_{\mathrm{CF}}^{(\mathrm{II})}$ with various $x_2 = \frac{B_{22}}{B_{20}}$

After the transformation of the $\mathcal{H}_{\mathrm{CF}}^{(\mathrm{II})}$ reference frame into its relevant PAS, this Hamiltonian becomes parameterizable with at most two CFPs $\left(B_{20}^{(i)}, B_{22}^{(i)}\right)$. Therefore, the diagram for the two-parameter orthorhombic form of $\mathcal{H}_{\mathrm{CF}}^{(\mathrm{II})}$, shown in figure 5, is fully representative for all orthorhombic, monoclinic and triclinic $\mathcal{H}_{\mathrm{CF}}^{(\mathrm{II})}$s. The question arises how to find this particular position of the reference frame for which such reduced parameterization becomes possible, i.e. exactly how to find the PAS (section 2). Below, some model orthorhombic coordinations are considered as an example. The initial symmetry-adapted reference system is co-axial with their relevant PASs. The functions $\left|B_{20}^{(i)}\right| / M_2$ of x_2 presented in figure 5 can be exemplified by the model orthorhombic $\mathcal{H}_{\mathrm{CF}}^{(\mathrm{II})}$s relevant to four ligands of the coordinates (in R units) as in figure 6: (1) $(\sin\theta\cos\phi, \sin\theta\sin\phi, \cos\theta)$; (2) $(-\sin\theta\cos\phi, \sin\theta\sin\phi, \cos\theta)$; (3) $(-\sin\theta\cos\phi, -\sin\theta\sin\phi, \cos\theta)$; (4) $(\sin\theta\cos\phi, -\sin\theta\sin\phi, \cos\theta)$. Then, taking into

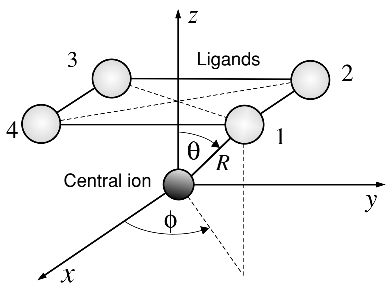

Figure 6. Model orthorhombic coordination of the central ion by four ligands, specified by the distance R and polar angular coordinates θ and ϕ.

account the point symmetry of the central ion surroundings and R^{-1} dependence of the individual ligand potential one gets

$$x_2 = \frac{B_{22}}{B_{20}} = \frac{-\sqrt{6}\sin^2\theta\cos 2\phi}{2(1-3\cos^2\theta)}. \tag{14}$$

Employing equation (14), the pivotal x_2 ratio can be assigned to the appropriate ligand rectangles (figure 6) specified by their θ and ϕ angles.

First of all, let us note that for $\phi = \frac{\pi}{4}$ the ratio x_2 equals zero irrespective of the θ angle, since such coordination corresponds to the tetragonal symmetry for which B_{22} vanishes except for $q = 0$ or $q = 4$. Besides, B_{20} CFP vanishes for $\theta = \arccos\frac{1}{\sqrt{3}} = 54.74^\circ$ and then in the limit $x_2 \to \infty$. In consequence, if $\theta = \arccos\frac{1}{\sqrt{3}}$ and $\phi = \frac{\pi}{4}$ both B_{20} and B_{22} become zero as the cubic symmetry conditions are obeyed.

Let us now analyse the case of $\theta = \frac{\pi}{2}$ and $\phi = \frac{\pi}{4}$, i.e. the square in the xy plane for which $x_2 = 0$ due to its tetragonal symmetry (figure 6). The ratio $x_2 = -\frac{\sqrt{6}}{2}$ corresponds to its two transformations, namely to the appropriate squares in the xz plane (rotating the initial square by $\left(0, \frac{\pi}{2}\right)$ angles) and in the yz plane (after the relevant rotation by $\left(\frac{\pi}{2}, \frac{\pi}{2}\right)$ angles). The positive value $x_2 = \frac{\sqrt{6}}{2}$ (equation (14)) refers to the alternative orientation of the initial square (i.e. $\phi = 0$). Therefore, this triad of the x_2 values $\left(0, \pm\frac{\sqrt{6}}{2}, \pm\frac{\sqrt{6}}{2}\right)$ corresponds to the three parameterizations of the $\mathcal{H}_{\mathrm{CF}}^{(\mathrm{II})}$ for the square of ligands placed perpendicularly to the three axes of the PAS, respectively. The magnitudes of $|B_{20}^{(i)}|\big/M_2$ for each x_2 from the triad are identical and equal to $1, \frac{1}{2}, \frac{1}{2}$, but they are assigned to the different plots of the diagram (figure 5). This is the case of $\mathcal{H}_{\mathrm{CF}}^{(\mathrm{II})}$ in the tetragonal symmetry surroundings which for the quadrupole is effectively axial.

Next, let us examine the case of the coordination rectangle with $\theta = \arccos\frac{1}{\sqrt{3}}$. As it results from equation (14) the B_{20} CFP is equal to zero, regardless of the ϕ angle (except for $\phi = \frac{\pi}{4}$) and consequently $x_2 \to \infty$. For $\phi = 0$, the considered rectangle reduces itself to the system of two double ligands in the xz plane (1 + 4 and 2 + 3 in figure 6) of the coordinates $\left(\pm R\sqrt{\frac{2}{3}}, 0, R\sqrt{\frac{1}{3}}\right)$, which is equivalent to the rectangle composed of four single ligands of the coordinates $\left(\pm R\sqrt{\frac{2}{3}}, 0, \pm R\sqrt{\frac{1}{3}}\right)$ and the ratio of the sides $\sqrt{2}$. As a result of both the rotations of the reference frame either by $\left(0, \frac{\pi}{2}\right)$ or $\left(\frac{\pi}{2}, \frac{\pi}{2}\right)$ angles the same $x_2 = \frac{1}{\sqrt{6}}$ is obtained. The alternative orientation of the initial rectangle (i.e. $\phi = \frac{\pi}{2}$) leads to $x_2 = -\frac{1}{\sqrt{6}}$. Thus, the obtained x_2 triads $\left(\infty, \pm\frac{1}{\sqrt{6}}, \pm\frac{1}{\sqrt{6}}\right)$ correspond indeed to the three equivalent parameterizations of $\mathcal{H}_{\mathrm{CF}}^{(\mathrm{II})}$ of the particular coordination rectangles described above.

Incidentally, for each of the three rectangles forming the icosahedron [19, 20] with the golden ratio of the sides $\frac{1}{2}(1+\sqrt{5})$, the relevant x_2 triad takes the values (5.186, 0.548, 0.289), however without any characteristic peculiarity.

5. Conclusions

For any $\mathcal{H}_{\mathrm{CF}}^{(\mathrm{II})}$ parameterization its PAS orientation with respect to the initial reference frame can be directly found based on equations (9) and (10). The rotational transformation of the initial parameterization into that referring to the PAS, i.e. its diagonalization, reduces the original, in general, five-parameter $\mathcal{H}_{\mathrm{CF}}^{(\mathrm{II})}$ with $x_1, x_2, \varphi_1, \varphi_2, B_{20}$, to one out of the three two-parameter $\mathcal{H}_{\mathrm{CF}}^{(\mathrm{II})}$ with $x_2^{(i)}, B_{20}^{(i)}$, where $i = 1, 2, 3$ denotes the axis of the PAS chosen as the z-axis of the system.

Within the PAS there are three equivalent two-parameter orthorhombic-like $\mathcal{H}_{\mathrm{CF}}^{(\mathrm{II})}$ parameterizations characterized by $x_2^{(i)} = B_{22}^{(i)} \big/ B_{20}^{(i)}$ ratios which are mutually correlated according to equation (13). Some definite relationships between the pairs of CFPs $B_{20}^{(i)}, B_{22}^{(i)}$ have been given (section 3).

Any choice of parameterization out of these three ones, e.g. that with maximal $\left|B_{20}^{(i)}\right|$ which is equivalent to that with the minimal value of $\left|x_2^{(i)}\right|$, is unambiguous for all the equivalent parameterizations.

In the case of the global $\mathcal{H}_{\mathrm{CF}}$ with its 2^k-pole components being rigidly coupled to each other, this unambiguous choice enables the standardization based on its quadrupolar components. There is no counterpart of the PAS for the higher order multipoles, but in the case of need a similar standardization could be based on the reference frames yielding, e.g., maximal values of B_{40} or B_{60} CFPs.

From among the three options of the z-axis within the PAS, for $i = 1, 2, 3$, always $\max\left|B_{20}^{(i)}\right| \big/ M_2 \geqslant 0.8660$ (figure 5) and the average value of the ratio within the typical range $|x_2| \leqslant 2$ exceeds 0.95. This fact suggests already a preliminary rough approximation possible at the beginning of the fitting procedure for $\mathcal{H}_{\mathrm{CF}}^{(\mathrm{II})}$—a parameterization pattern with only one non-zero second-order CFP, i.e., B_{20}.

The question about the physical grounds for such specific orientation of the PAS with respect of the crystallographical reference system remains open. It seems to be particularly intriguing for triclinic surroundings where no directions are preferred at all. In other words, what is the physical sense of the second-order $\mathcal{H}_{\mathrm{CF}}^{(\mathrm{II})}$ diagonalization. Undoubtedly, the correlation between the principal axes and the distinguished points on the $B'_{20}(\alpha, \beta)$ map, i.e., its maximum, minimum and saddle point, is a hint approaching the answer.

References

[1] Wybourne B G 1965 *Spectroscopic Properties of Rare Earths* (New York: Wiley)

[2] Rudowicz C 1987 *Magn. Reson. Rev.* **13** 1

[3] Rudowicz C and Qin J 2004 *J. Lumin.* **110** 39

[4] Morrison C A and Leavitt R P 1982 Spectroscopic properties of triply ionized lanthanides in transparent host crystals *Handbook of the Physics and Chemistry of Rare Earths* ed K A Gschneidner and L Eyring Jr (Amsterdam: North-Holland) pp 461–692

[5] Newman D J and Ng B 2000 *Crystal-Field Handbook* ed D J Newman and B Ng (Cambridge, MA: Cambridge University Press)

[6] Mulak J and Gajek Z 2000 *The Effective Crystal-Field Potential* (Amsterdam: Elsevier) chapter 2

[7] Rudowicz C 1986 *J. Chem. Phys.* **84** 5045
[8] Rudowicz C and Bramley R 1985 *J. Chem. Phys.* **83** 5192
[9] Rudowicz C 1985 *Chem. Phys.* **97** 43
[10] Rudowicz C and Qin J 2003 *Phys. Rev.* B **67** 174420
[11] Abragam A and Bleaney B 1970 *Electron Paramagnetic Resonance of Transition Ions* (Oxford: Clarendon)
[12] Rudowicz C and Misra S K 2001 *Appl. Spectrosc. Rev.* **36** 11
[13] Edmonds A R 1960 *Angular Momentum in Quantum Mechanics* (Princeton, NJ: Princeton University Press)
[14] Burdick G W and Reid M F 2004 *Mol. Phys.* **102** 1141
[15] Mulak J and Mulak M 2005 *J. Phys. A: Math. Gen.* **38** 6081
[16] Gajek Z, Mulak J and Krupa J C 1993 *J. Solid State Chem.* **107** 413
[17] Hamermesh M 1989 *Group Theory and Its Application to Physical Problems* (New York: Dover)
[18] Rudowicz C and Sung H W 2003 *Physica* B **337** 204
[19] Altshuler S and Kozyrev B M 1974 *Electron Paramagnetic Resonance in Compounds of Transition Elements* (New York: Wiley)
[20] Judd B R 1957 *Proc. R. Soc.* A **241** 122